Advance Publication Cover Page

Chemistry Letters

Multi-Response Quinoxaline-Based Fluorophores: Solvatochromism, Mechanochromism, and Water Sensoring

Jia Yu, Zhifang Liu, Bowei Wang,* Yuqi Cao, Dongqi Liu, Yixian Wang, and Xilong Yan*

Advance Publication on the web November 12, 2019

doi:10.1246/cl.190732

Multi-Response Quinoxaline-Based Fluorophores: Solvatochromism, Mechanochromism, and Water Sensoring

Jia Yu,[a1] Zhifang Liu,[a1] Bowei Wang,*[1,2,3] Yuqi Cao,[1] Dongqi Liu,[1] Yixian Wang,[1] and Xilong Yan*[1,2,3]
[1]*School of Chemical Engineering and Technology, Tianjin University, Tianjin, 300350, P. R. China.*
[2]*Collaborative Innovation Center of Chemical Science and Engineering (Tianjin), Tianjin, 300072, P. R. China.*
[3]*Tianjin Engineering Research Center of Functional Fine Chemicals, Tianjin, P. R. China*
[a]*These authors contributed equally to this work.*

E-mail: yan@tju.edu.cn (Xilong Yan), bwwang@tju.edu.cn (Bowei Wang)

Three new D-π-A type quinoxaline-cored fluorophores were elaborately designed and synthesized. It was found that P-1, P-2, and P-3 (Ps) all presented bathochromic-shifted mechanochromic (MFC) natures upon grinding, accompanied with 30 nm, 8 nm, and 37 nm red-shift, respectively. The DSC and PXRD were recorded to reveal the mechanism of the MFC process. Moreover, P-1 is sensitive to water in tetrahydrofuran (THF), acetonitrile (MeCN) and acetone with a detection limit of 0.12%, 0.0078%, and 0.0110%, respectively. This work provided a rational strategy for developing multi-responsive fluorescence materials.

Keywords: Multi-stimuli-responsive, Water detection, Structure-function relationship

Organic fluorophores response to external force stimuli have received extensive attention for their potential applications as security ink,[1] fluorescent chemosensors,[2,3] and optical materials,[4,5] and tremendous efforts have been devoted to stimuli-responsive fluorophores, such as mechanochromic materials and water probes.[6-11] There already have been some reports concerned with organic water sensors.[12] However, few organic molecules possess the MFC, solvatochromic, and water sensoring properties at the same time. In addition, most reported organic water sensors are able to detect water for H-bond acceptor effect or twisted intramolecular charge transfer (TICT) mechanism, and almost none of them acted as a H-bond donor in the water sensoring process. Moreover, the reported water detection mechanism is mostly based on density functional theory (DFT) calculation and few direct evidences have been provided.

In this work, we introduced the P-1 based on 2, 3-dimethylquinoxaline template, which is a mechano- and solvatochromic material as well as a water-sensitive material. Moreover, we developed another two quinoxaline-cored fluorophores for comparison with P-1, and named as P-2 and P-3 (Scheme 1). Furthermore, DFT calculation and crystal data were provided for detailed investigation of internal influence factors of water sensing and MFC properties.

The synthesis routes and the characterization of these Ps are illustrated in supporting information. As illustrated in Figure S4, the absorption spectra of Ps displayed two absorption peaks. The absorption peaks in the shorter and longer wavelength region are attributed to π-π* transition at aromatic rings and the whole molecules, respectively.

Considering their D-π-A structures, the PL spectra were characterized in five solvents with different polarity. These compounds displayed significant red-shifted solvatochromism, in which P-1, P-2, P-3 exhibited spectra shift from 457 nm, 447 nm, 497 nm in *n*-hexane to 557 nm, 505 nm, 537 nm in DMF, respectively, along with 100 nm, 58 nm, 40 nm red-shifts. (Figure S4) In general, the polar solvents have a better stabilization effect on the excited state during π-π* transition process. As a result, the energy gap gets narrower with the increase of solvent polarity, accompanied with red-shifted PL spectra.[13,14]

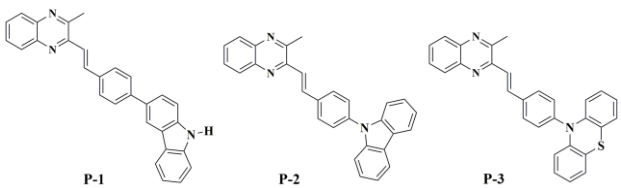

Scheme 1. Chemical structures of Ps.

Moreover, the Lippert-Mataga equation, which relates the Stokes shift (Δυ) with solvent orientation polarizability, was employed to evaluate the solvatochromism of Ps. It's obvious that P-1 shows distinct solvatochromic property with the largest slope of fitting line. (Figure S5) Usually, molecules with such outstanding solvatochromic red-shift and excellent linearity in different solvents can be applied as a water sensor in organic solvents.[15]

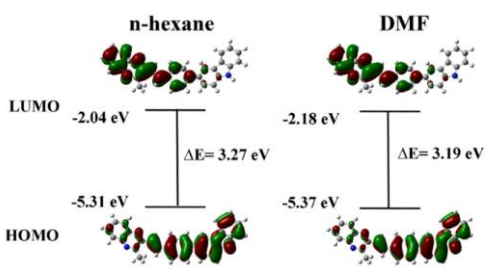

Figure 1. Molecular orbital amplitude of P-1 in *n*-hexane and DMF solution

As to gain a further understanding of the distinct ICT effect of P-1, DFT calculation was carried out and illustrated in Figure 1. The HOMO orbitals of P-1 were distributed over the whole molecule, while the LUMO orbitals were mainly concentrated on the quinoxaline and

neighboring benzene ring, indicating well charge separated D-π-A structure. In addition, the energy gap was 3.27 eV in *n*-hexane solution and decreased to 3.19 eV in DMF, attributing to the more stabilized excited state in polar solvents. Consequently, the emission peaks shifted toward the long wavelength area in polar solvents.[15]

Furthermore, the calculation of P-1-water hydrogen bonding association was also employed to clarify the water sensing ability of P-1. As illustrated in Figure S6, when P-1 was bonded with water molecule (P-1-H_2O), the energy level of both HOMO (−5.07 eV) and LUMO (−1.88 eV) was obviously driven down, contributing to a narrower energy gap (3.19 eV) compared to the isolated molecule (3.33 eV), which led to an enhanced ICT effect. As a result, the PL intensity experienced a dramatically decrease along the addition of water.

On the basis of the above discussion, it is possible for P-1 to present water sensitive behavior in organic solvents. Thus, further study was carried out. The PL spectra of P-1 in THF, MeCN, and acetone with water fraction vary from 0% to 10% were illustrated in Figure 2. Typically, the emission intensity of P-1 experienced a dramatically decrease tendency along with slight bathochromic shift with the addition of water. When water fraction (f_w) reached up to 1.0%, the emission intensity of P-1 descended to 30% in MeCN and a drastic decrease to 2% at f_w = 10%. Meanwhile, the PL intensity correlated well with f_w, exhibiting perfect linearity. Unsurprisingly, water sensor experiments presented the same downtrend in THF and acetone. Furthermore, the detection limits of P-1 in these organic solvents were calculated with 3σ/k method.[14,16] (σ refers to the standard deviation of the blank signal, and k represents the slope of PL intensity vs water fraction) The calculated detection limits were 0.12%, 0.0078% and 0.0110% for P-1 in THF, MeCN, and acetone respectively. Compared with the previously reported fluorescence water sensors, the detection limit of P-1 in MeCN is standout among them. (Table S1) Consequently, it is reasonable that P-1 can be employed as an ultrasensitive water sensor in some types of organic solvents.

According to Lu et al,[13] nonplanar D-A type π conjunction molecules can exhibit MFC behavior and their mechanochromism is anticipated. As illustrated in Figure 3, the emission color of pristine P-1, P-2, and P-3 switched from green, blue, and yellow to yellow, blueish-green, and pale-orange by grinding, accompanied with 30 nm, 8 nm, and 37 nm red-shift, respectively. And they show reversible mechanochromic process by annealing. After grinding, the fluorescence quantum yield (Φ_F) of P-1 is decreased from 50% to 37% and the lifetime (τ) of P-1 is prolonged from 5.27 μs to 6.23 μs. (Table S2) Both P-2 and P-3 show similar phenomenon. Before and after grinding, there are obvious changes in the radiative decay rates (k_r) and non-radiative decay rates (k_{nr}) for Ps. ($k_r = \Phi_F/\tau$, $k_{nr} = (1-\Phi_F)/\tau$).[17] Therefore, grinding might alters the fluorescence emission channels. The Φ_F of Ps are decreased after grinding, which is attributed to the increased k_{nr} or reduced k_r by grinding.[1]

As we know, the MFC behavior always has an inherent relationship with their staking modes transformation during the grinding process.[18] To determine the MFC mechanism, PXRD of these molecules were studied. As demonstrated in Figure 4, pristine samples exhibited sharp and strong curves, indicating well-ordered structure.

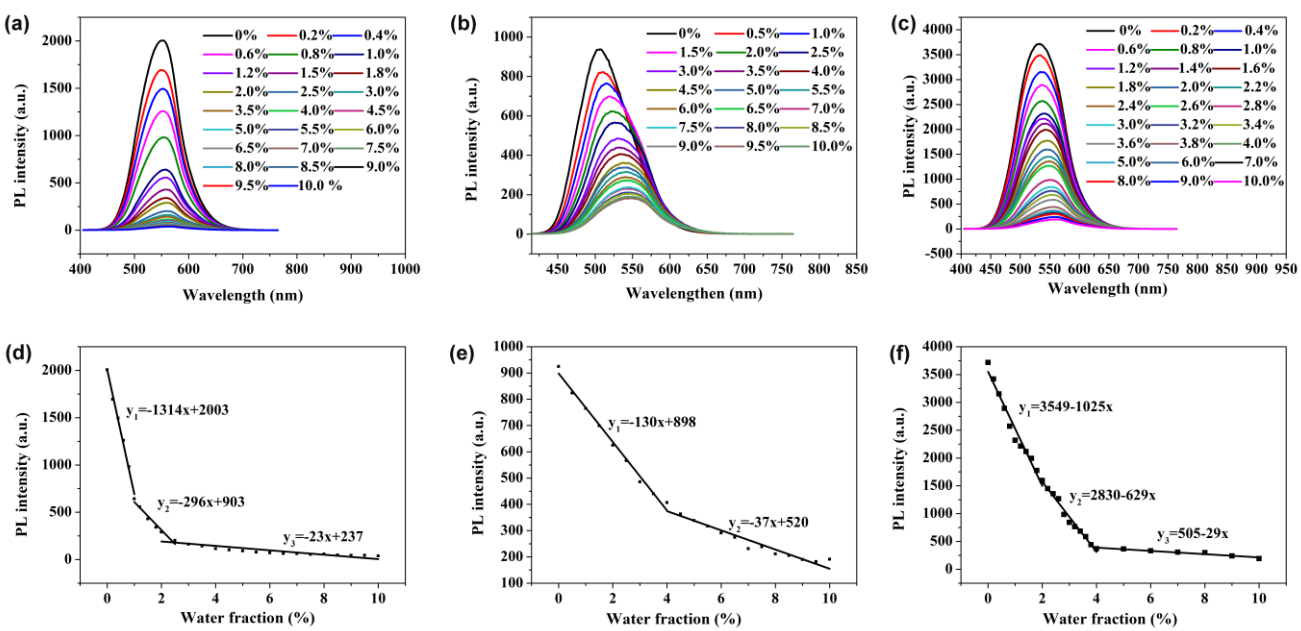

Figure 2. PL spectra of P-1 in (a) MeCN, (b) THF and (c) acetone with different amounts of water (from 0% to 10%, v/v). Plots of the PL intensity of P-1 with different water contents in (d) MeCN, (e) THF and (f) acetone.

.

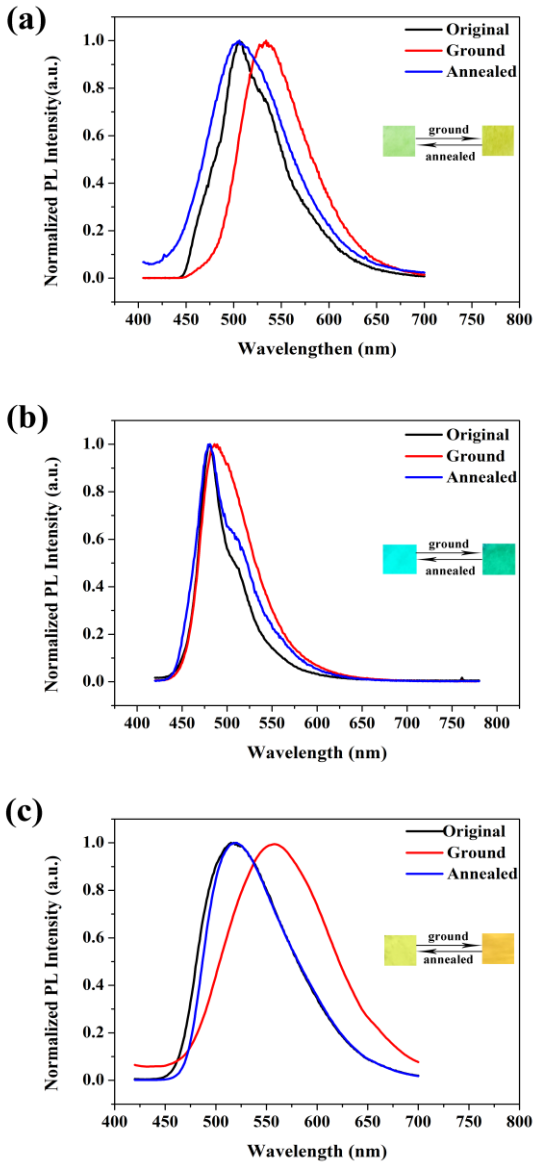

Figure 3. Normalized PL spectra in solid states of the original, ground and annealed samples. (a) P-1; (b) P-2; (c) P-3.

Upon grinding, some sharp peaks of P-1 and P-3 got broader or even disappeared while the spectra of P-2 experienced minor change. Moreover, some new peaks appeared in the curves of P-1. The disappeared or broader peaks of P-3 indicated a morphological transition from well-order crystalline phases to disordered amorphous structures.[9] These new peaks of P-1 also suggested a packing mode transformation from one crystal state to another. As for P-2, we supposed its' crystal structure experienced little packing mode change.[13] In general, grinding of the sample sometimes cause solid-solid phase transitions, and the rupture or the formation of new intermolecular interactions, maintaining the crystalline order. To understand the thermo properties of these three compounds, the DSC and TGA results were recorded and illustrated in Figure S7. The original samples of P-2 displayed one endothermic peak in the high temperature-zone, originated from the isotropic melt transition (T_m). (Figure S7) As for the ground P-2, it exhibited an extra endothermic peak at a relatively low temperature at 50 °C, which might refer to as the solid-solid phase transition. Different from P-2, an extremely weak endothermic peak was observed at 100 °C in P-1 and P-3.

In order to further understand the correlation between structures and MFC functions, we prepared crystals by slow diffusion of MeCN into a saturated CH_2Cl_2 solution of complexes. Finally, we got the single crystals of P-2, P-3, and co-crystal with MeCN of P-1 (crystal model has been squeezed).[1] The crystal data were illustrated in Table S3, Table S4, and Table S5. All these crystals belong to the monoclinic system and adopted a loose *J*-type packing modes, leading to structural defects and low lattice energy.

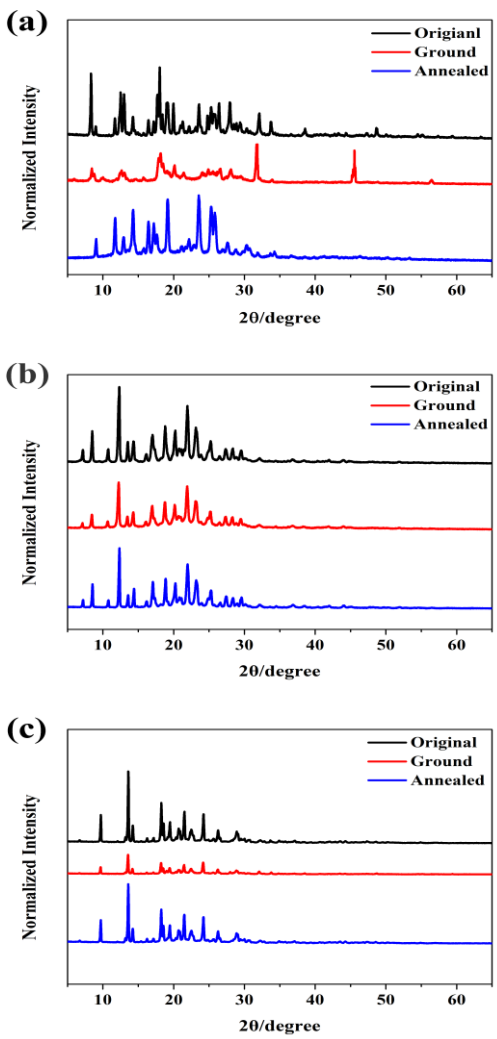

Figure 4. XRD spectra of the original, ground and annealed samples of (a) P-1, (b) P-2 and (c) P-3.

The co-crystal of P-1 indicated the hydrogen bond interaction with water and other hydrogen bond acceptor solvents. Meanwhile, the torsion angles of the linked

benzene ring between quinoxaline and the carbazole moiety were 18.19° and 29.92°, respectively. As for P-2 and P-3, the dihedral angle and torsion angle was 44.91° and 82.28°, respectively (torsion angle between the linked benzene ring and quinoxaline was small enough to be negligible). (Figure 5)

Moreover, it was hard to find π-π interaction in the crystal of P-1 and P-2. However, in the crystal of P-3, one-dimensional π-π interaction occurred, with a distance of 3.414 Å. Upon grinding, the binding energy released and the crystal structures were destroyed, leading to the slipping of adjacent molecular layers and decreased dihedral angle.[7,19] However, the crystal structure of P-2 could recover to a certain degree for the absence of the π-π interaction.[19,20] As a result, the ground P-3 displayed the largest emission shift, while P-2 presented minor spectra red-shift upon grinding.

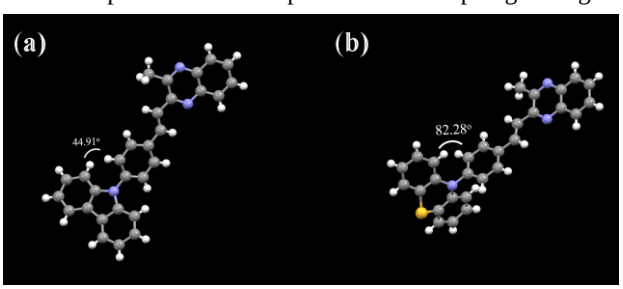

Figure 5. The configurations of (a) P-2 and (b) P-3.

In this work, three D-π-A type multi-responsive materials were designed and synthesized. These compounds exhibited distinct solvatochromism, in which P-1 exhibited the largest spectra shift (λs = 100 nm). In addition, the outstanding ICT effect and hydrogen bond effect with water enabled P-1 sensitive to water in THF, MeCN and acetone with a detection limit of 0.12%, 0.0078% and 0.0110%, respectively. Upon addition of water in the organic solvents of P-1, hydro-bond formed, which led to an enhanced ICT process. Thus, the emission intensity decreased as a result, enabling water detecting probability. In addition, the hydrogen bond interaction was further proved by the co-crystal of P-1 with MeCN. Moreover, Ps also presented vary degrees of mechanochromism and explained by single crystals as well as XRD and DSC results. Among them, P-3 exhibited the most distinct mechanochromism for its most twisted structure and crystal-amorphous transformation up grinding. As for P-2, the minor MFC red-shift might be attributed to little phase transformation during the grounding process. Notably, our work reported an organic water sensor molecule for H-bond donor mechanism and provided a rational strategy for the design of multi-response organic materials.

This work was financially supported by the National Natural Science Foundation of China (Grant No. 21576194)

Supporting Information is available on http://dx.doi.org/10.1246/cl.******.

References and Notes

1 Z. Wu, S. Mo, L. Tan, B. Fang, Z. Su, Y. Zhang, M. Yin, *Small* **2018**, *14*, 1802524.

2 E. Kim, A. Podder, M. Maiti, J. M. Lee, B. G. Chung, S. Bhuniya, *Sens. Actuators B Chem.* **2018**, *274*, 194.

3 Y. Zhang, L. Yuan, S. Jia, X. Liu, J. Zhao, G. Yin, *Phys. Chem. Chem. Phys.* **2019**, *21*, 3218.

4 B. Xu, Y. Mu, Z. Mao, Z. Xie, H. Wu, Y. Zhang, C. Jin, Z. Chi, S. Liu, J. Xu, Y. Wu, P. Lu, A. Lien, M. R. Bryce, *Chem. Sci.* **2016**, *7*, 2201.

5 M. Okazaki, Y. Takeda, P. Data, P. Pander, H. Higginbotham, A. P. Monkman, S. Minakata, *Chem. Sci.* **2017**, *8*, 2677.

6 H. Gao, P. Xue, J. Peng, L. Zhai, M. Sun, J. Sun, R. Lu, *New J. Chem.* **2019**, *43*, 77.

7 Y. Xiong, X. Yan, Y. Ma, Y. Li, G. Yin, L. Chen, *Chem. Commun.* **2015**, *51*, 3403.

8 Y. Cao, W. Xi, L. Wang, H. Wang, L. Kong, H. Zhou, J. Wu, Y. Tian, *RSC Adv.* **2014**, *4*, 24649.

9 Z. Chang, L. Jing, C. Wei, Y. Dong, Y. Ye, Y. S. Zhao, J. Wang, *Chem. Eur. J.* **2015**, *21*, 8504.

10 Y. Shen, P. Chen, J. Liu, J. Ding, P. Xue, *Dyes Pigments* **2018**, *150*, 354.

11 P. Xue, Z. Yang, P. Chen, *J. Mater. Chem. C* **2018**, *6*, 4994.

12 K. Nishino, H. Yamamoto, J. Ochi, K. Tanaka, Y. Chujo, *Chem. Asian. J.* **2019**, *14*, 1577.

13 P. Xue, B. Yao, J. Sun, Q. Xu, P. Chen, Z. Zhang, R. Lu, *J. Mater. Chem. C* **2014**, *2*, 3942.

14 L. Ding, Z. Zhang, X. Li, J. Su, *Chem .Commun.* **2013**, *49*, 7319.

15 X. Guan, T. Jia, D. Zhang, Y. Zhang, H. Ma, D. Lu, S. Lai, Z. Lei, *Dyes Pigments* **2017**, *136*, 873.

16 T. Chen, Z. Chen, W. Gong, C. Li, M. Zhu, *Mater. Chem. Front.* **2017**, *1*, 1841.

17 M. Chen, R. Chen, Y. Shi, J. Wang, Y. Cheng, Y. Li, X. Gao, Y. Yan, J. Sun, A. Qin, R. Kwok, J. Lam, B. Tang, *Adv. Funct. Mater.* **2018**, *28*, 1704689.

18 a) Y. Xi, Y. Cao, Y. Zhu, H. Guo, X. Wu, Y. Li, B. Wang, *Chem. Lett.* **2018**, *47*, 650. b) K. Suenaga, K. Tanaka, Y. Chujo, *Eur. J. Org. Chem.* **2017**, *2017*, 5191. c) K. Suenaga, K. Tanaka, Y. Chujo, *Chem. Eur. J.* **2017**, *23*, 1409. d) Y. Gong, Y. Zhang, W. Yuan, J. Sun, Y. Zhang, *J. Phys. Chem. C* **2014**, *118*, 10998.

19 J. Xiong, K. Wang, Z. Yao, B. Zou, J. Xu, X. Bu, *ACS Appl. Mater. Interfaces* **2018**, *10*, 5819.

20 C. Ma, B. Xu, G. Xie, J. He, X. Zhou, B. Peng, L. Jiang, B. Xu, W. Tian, Z. Chi, S. Liu, Y. Zhang, J. Xu, *Chem. Commun.* **2014**, *50*, 7374.